



Gas-filled membrane absorption: a review of three different applications to describe the mass transfer by means of a unified approach

Ayça Hasanoğlu^{a,b}, Julio Romero^{a,*}, Andrea Plaza^a, Wladimir Silva^a

^aLaboratory of Membrane Separation Processes (LabProSeM), Department of Chemical Engineering, University of Santiago de Chile (USACH), Santiago, Chile

Tel. +56 2 718 18 21; email: julio.romero@usach.cl

^bDepartment of Chemical Engineering, Yıldız Technical University, Davutpaşa, Istanbul 34210, Turkey

Received 19 July 2012; Accepted 10 December 2012

ABSTRACT

This work involves the presentation of a general approach to describe the gas-filled membrane absorption process by analyzing three different applications. Ammonia removal from wastewater was described in a previous work using a resistance-in-series model. In this contribution, this model has been applied to describe the HCN removal from wastewater as well as to characterize the transfer of SO₂ from wines to a receiving solution to develop a new method for enhanced quantification of sulfite content. The experimental results of this novel technique for SO₂ quantification and its theoretical validation are presented in this study. The analyzed operations are based on hydrophobic hollow fiber contactors, which are used to physically separate two aqueous phases: a feed solution containing a volatile compound and a reactive receiving solution. Mainly removal of three volatile compounds under this configuration was analyzed: NH₃, HCN, and SO₂. By this way, a unified description based on a resistance-in-series model was developed for the three chemical absorption systems, obtaining good agreement between experimental data and the predicted values. Furthermore, the extraction percentages were significantly high (up to 99.9%) for the three systems. The mass transfer model shows a significant influence of the hydrodynamic conditions of the feed solution, gas solubility, and the rate of reaction on the performance of the process.

Keywords: Membrane absorption; Mass transfer; Modeling; Ammonia; HCN; SO₂

1. Introduction

The removal and recovery of dissolved gases from liquids have started posing a challenge, particularly due to increasing levels of environmental pollution. Stricter regulations were established in many countries for the removal of pollutants from the

wastewater streams. Removal of dissolved components of gases and volatile compounds is also an emerging issue for several industries to enhance the product quality such as liquid food and electronic industries, as well as being an emerging issue for wastewater treatments. Several techniques are available for dissolved gas and volatile compound removal including adsorption, absorption, advanced oxidation,

*Corresponding author.

incineration, and biological treatment [1–3]. However, most of these techniques not only require high capital and operational costs and the limitation of the feed condition in actual application, but also produce a problem of post-treatment. Furthermore, most of these applications are limited in bringing down the contaminant concentration in the treated stream to very low levels. Membrane contactors are gradually used to replace conventional methods [4,5]. Membrane contactors usually utilize macroporous hollow fiber membrane as an interface to separate gas and liquid phases, and thereafter achieve the mass transfer from one phase to another phase. Absorption of gaseous components into receiving liquids is identified as gas–liquid type mass transfer, which is called membrane gas absorption. To perform the gas absorption in such a design based on a membrane contactor has a number of unique advantages over a classical absorber; it offers large surface area for mass transfer, provides flexible and compact design, which is easy to monitor and adapt to existing systems.

In this paper, the use of membrane gas absorption with a reactive strip solution is analyzed for removal of dissolved gases from aqueous streams. Here, the volatile species reacts with a component in the receiving phase. Thus, the activity and vapor pressure of the species to be separated is lowered in the receiving

solution resulting in enhancement of the driving force necessary for the mass transfer. Fig. 1 shows an outline of the gas-filled membrane absorption process described in this work.

The mass transfer of the solute S through the membrane is achieved by means of the following sequence of steps indicated on the Fig. 1:

- (1) Transfer through the boundary layer of aqueous feed solution to be treated;
- (2) Phase equilibrium between the feed solution and the gas phase retained in the membrane pores;
- (3) Mass transfer of the volatile solute S through gas-filled gap;
- (4) Phase equilibrium between the gas phase and the receiving solution. The formation of an absorbed compound at the interface can be considered in this step;
- (5) Mass transport of absorbed compound in the receiving solution through its boundary layer.

Since the macroporous polypropylene membrane is hydrophobic, the membrane will not allow liquid water to pass through the pore and thus it separates physically two aqueous streams resulting in an immobilized gas–liquid interface at both membrane

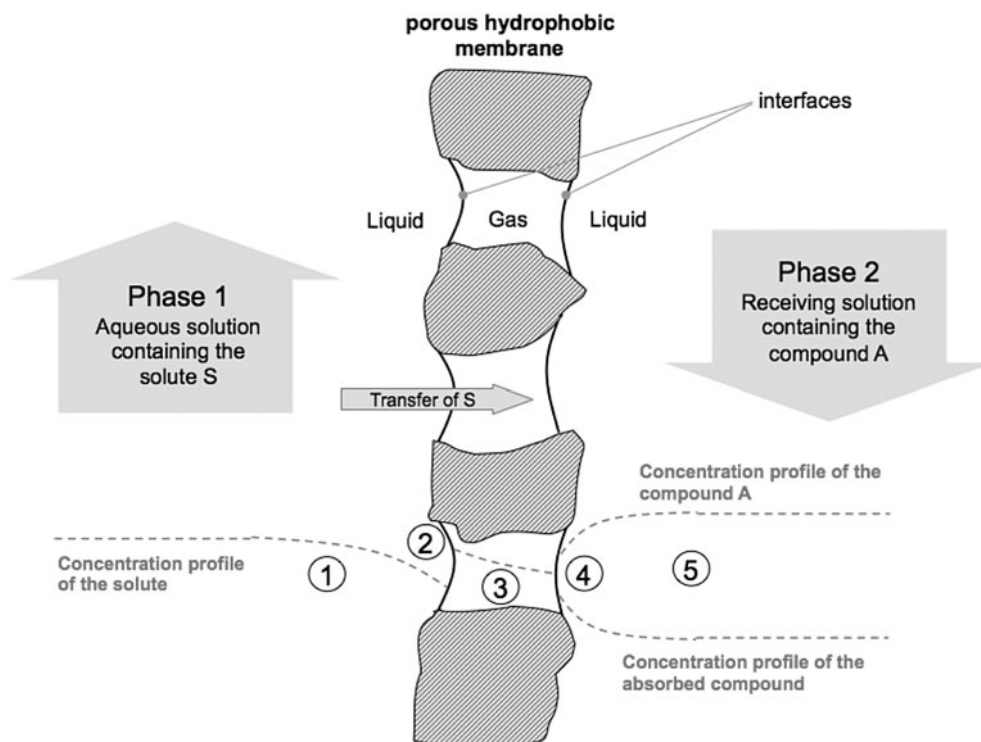


Fig. 1. General outline of a membrane absorption process.

Table 1
Membrane absorption systems and their operating parameters analyzed in this work

System	Application	Phases		Compound generated in the receiving solution	Experimental	Theoretical	Studied operation parameters	Intervals	Units
		Phase 1	Phase 2						
1	Ammonia removal from water	NH ₃ aqueous solution	Porous and hydrophobic membrane	Diluted H ₂ SO ₄ solution	[9]*	[9]*	Temperature	35–50	°C
					[28]	[28]	Feed concentration	250–500	ppm
					[29]	[29]	Receiving solution concentration	0.1–0.3	mol L ⁻¹
2	HCN removal from wastewater	HCN aqueous solution	Porous and hydrophobic membrane	NaOH or KOH solution	[10]	This work	Temperature	20	°C
					[11]*	[12]	Feed concentration	1277.5	mg L ⁻¹
					[12]		Receiving solution concentration	10	% (wt)
3	SO ₂ quantification from wines and fruit juices	Wine or fruit juice	Porous and hydrophobic membrane	NaOH solution	[13]		Flow rate of the solutions	500	mL min ⁻¹
					This work	This work	Volume of feed	1,000	mL
							Temperature	25–27	°C
							Feed concentration	160–210	ppm
							Receiving solution concentration	0.02	mol L ⁻¹
							Flow rate of the solutions	1.20–1.45	L min ⁻¹
							Volume of feed	300	mL
							Volume of receiving solution	300	mL

Note: *Cases to be analyzed in this contribution.

surfaces. The polarity difference between polypropylene and water is high and for that reason water is a non-wetting fluid for the polypropylene membrane at normal conditions. A non-wetting fluid does not penetrate into the pores as long as the pressure on the non-wetting side is kept below some critical value known as breakthrough pressure. This breakthrough pressure for water–polypropylene membrane system is given as 11.3 bar by Wiesler [6], and this value is much higher than the pressure of the aqueous streams used in the experiments. The equation for breakthrough pressure is given below:

$$\Delta P = 2(\sigma \cos \theta)/r \quad (1)$$

Here, σ is the surface tension, θ is the contact angle, and r is the pore radius. The contact angle is the angle formed between the fluid and the membrane pore. This angle increases with increasing polarity difference between the membrane material and the fluid. Higher contact angle is an indicative to a higher polarity difference between fluid and membrane material. Thus, this parameter can be used to describe the hydrophobicity of a surface and its resistance to pore wetting. Lv and coworkers [7] studied wetting of polypropylene membranes and showed that contact angle of the water–polypropylene system was 107° after 30 days of immersion of the fibers in water. This value is over 90° , which indicates that the surface is still hydrophobic after 30 days of immersion. Thus, in this study, the pores of the membrane are assumed as non-wetted by aqueous phases.

This configuration presents several advantages in terms of the local and global mass transfer at the proximities of the membrane. The effect of the membrane on the overall mass transfer resistance is not extremely significant considering the thickness of the gas gap, which could be between 20 and $40 \mu\text{m}$

according to previous work reported in the literature [8–14]. The use of hollow fiber contactors represents many technical advantages over other processes, since the high value of specific contact surface area (m^2/m^3) of these membrane modules involves a high volumetric efficiency of the operation. Several authors [15–22] describe various applications of hollow fiber contactors.

On the other hand, the presence of the chemical reaction in the receiving phase reduces drastically the overall transfer resistance of the solute. In terms of the driving force of the process, the conversion of the solute S in the receiving phase increases the extraction efficiency and accelerates its transport rate.

One of the most important limitations of this configuration is related to the hydrodynamic conditions in the membrane modules used for these applications, since the geometry of the hollow fiber contactors involves the circulation of solutions under laminar flow with extremely low Reynolds numbers, which represent low mass transfer coefficient values in the boundary layers at the proximities of the membrane. Modifications in the design of these modules could solve partially those limitations, but these aspects will not be developed in this contribution.

Table 1 summarizes the three study cases to be analyzed in this work. These three different applications are related to the treatment of waste or process waters and liquid foods or beverages.

2. Applications

2.1. General description of the method

The membrane contactors employed in the analyzed works were hollow fiber modules consist of polypropylene fibers. Table 2 presents the structural parameters of the fibers.

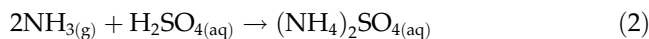
Table 2
Structural parameters of the hollow fiber contactors used in experiments for each analyzed case

Parameter, unit	Interval of values		
	NH ₃ removal [9]	SO ₂ quantification (this work)	HCN removal [11]
Hollow fiber membrane module	Celgard Liquicel [®]	Celgard Liquicel [®]	Selfmade
Membrane material	Polypropylene	Polypropylene	Polypropylene
Number of fibers	7,400	7,400	600
Surface contact area, m ²	0.58	0.58	0.1444
Fiber O.D., μm	300	300	426
Fiber I.D., μm	220	220	336
Mean pore diameter, μm	0.2	0.2	0.05
Length, m	0.12	0.12	0.18

In each application, a reactive stripping solution were used that was circulated into the shell or lumen-side of the hollow fiber module while the aqueous feed solution containing the volatile species was circulated through other side of the module by using two different pumps. Both solutions were recycled to their respective reservoirs in order to be re-circulated through the membrane. At regular time intervals, the concentration of the feed solution was monitored.

2.2. Ammonia removal from water

In our previous work, removal of ammonia from industrial effluent was investigated by means of gas-filled membrane absorption in order to investigate the optimum process parameters [9]. In the present work, this case is analyzed on the basis of a unified approach comparing other applications of gas-filled membrane absorption. Diluted solution of sulfuric acid was used as a receiving solution to accelerate the removal of ammonia by means of a reaction converting the ammonia into ammonium sulfate ((NH₄)₂SO₄), which could be recovered as a by-product. Here, the corresponding chemical absorption reaction is as follows:



Feed solution was recycled through shellside of the membrane. Fig. 2 shows a general description of the experimental setup for ammonia removal application. The concentration of NH₃ was monitored by means of

a ion-selective electrode, which remained immersed in the feed aqueous solution during the experiment.

2.3. Recovery of cyanide from wastewater

Cyanide removal by means of gas-filled membrane absorption was reported in the literature [10–13]. The case analyzed here for the cyanide removal was an integrated process of coagulation and gas membrane absorption for the treatment of praziquantel wastewaters reported by Xu and coworkers [11]. Praziquantel is an anti-schistosoma drug that is used in pharmaceutical industries. The major pollutants in praziquantel manufacturing wastewater are cyanide and other by-products. HCN dissociates in aqueous solutions. Under acidic to neutral conditions, cyanide is present as HCN. Since HCN is the species that diffuses through the membrane, the pH of the feed solution must be adjusted in order to obtain HCN form of the cyanide. The original praziquantel wastewater had a pH value between 9.5–10 and contained 1,000–3,500 mg L⁻¹ CN⁻. In the above-mentioned study, cyanide removal was carried out using original and artificial praziquantel wastewaters adjusting the pH of the feed below 6 using HCl solution. The feed solution was treated with 10% KOH solution by means of a gas-filled membrane absorption process. The cyanide in the wastewater was recovered in the receiving phase. The corresponding reaction occurred was as follows:

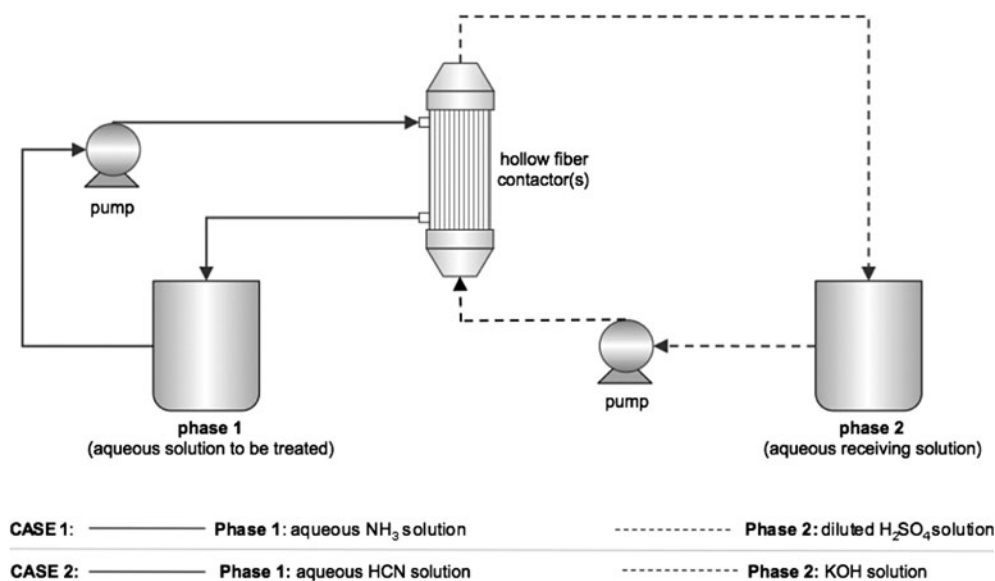
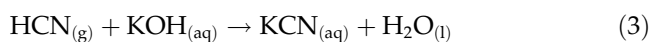


Fig. 2. General outline of the gas-filled membrane absorption process for ammonia and HCN removal.

Since the praziquantel wastewater has turbidity, the wastewater was pretreated by coagulation. Three types of feed solutions were investigated using gas-filled membrane absorption: artificial, coagulated, and uncoagulated wastewaters. In this paper, the case with artificial wastewaters was analyzed in terms of the unified approach. Acidified feed solution and 10% KOH of strip solution flowed in lumenside and shell-side, respectively. The same configuration described in Fig. 2 can be considered for this application.

2.4. SO₂ removal from wines and fruit juices

The main principles of sulfite quantification using gas-filled membrane absorption for SO₂ control in wines was described by Plaza and coworkers [14]. Here, the experimental results and its theoretical validation is presented and analyzed. Sulfur dioxide is a preservative widely used in fruit-derived products. In

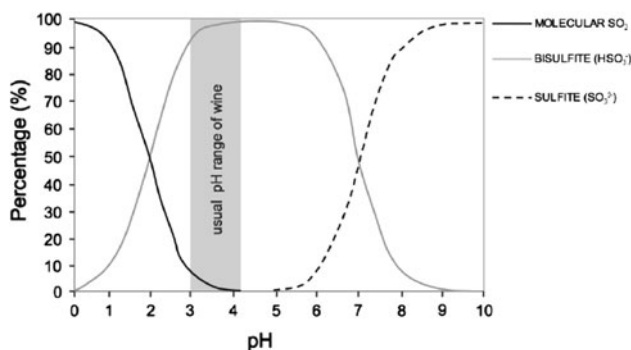
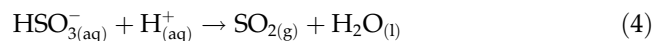


Fig. 3. Distribution percentages of chemical species in wine depending on the pH value.

the reported study, it was proposed to use a gas-filled membrane absorption process for selective removal or recovery of sulfites from wines or other liquid foods in order to obtain a reliable quantification of these compounds. The feed solution containing red wine was acidified using a H₂SO₄ solution in order to ensure the formation of sulfites in the volatile form since the presence of volatile SO₂ increases with decreasing pH values. The receiving solution used for this process was 0.02 M NaOH solution. The case analyzed for sulfite quantification is based on extraction of free and bounded sulfite content from wine by modifying the pH value to extract the non-volatile forms (HSO₃⁻ and SO₃²⁻) converting them into volatile form, SO₂. In this way, the volatile form, SO₂ is transferred through the membrane contactor and recovered as a sulfite in the receiving solution. The reaction occurred by acidification is as follows:



As the bisulfite is converted to SO₂, it is absorbed in the receiving solution of NaOH and then reacts with NaOH where absorbed SO₂ becomes SO₃²⁻:



Fig. 3 presents an outline with the molar percentage of each compound dissolved in wine as a function of the pH. At usual values of pH, bisulfite and sulfur dioxide may be identified in the wine, but at lower pH values, the presence of sulfur dioxide increases. Thus, the pH value of the feed is an important variable on the process, since only the volatile form of

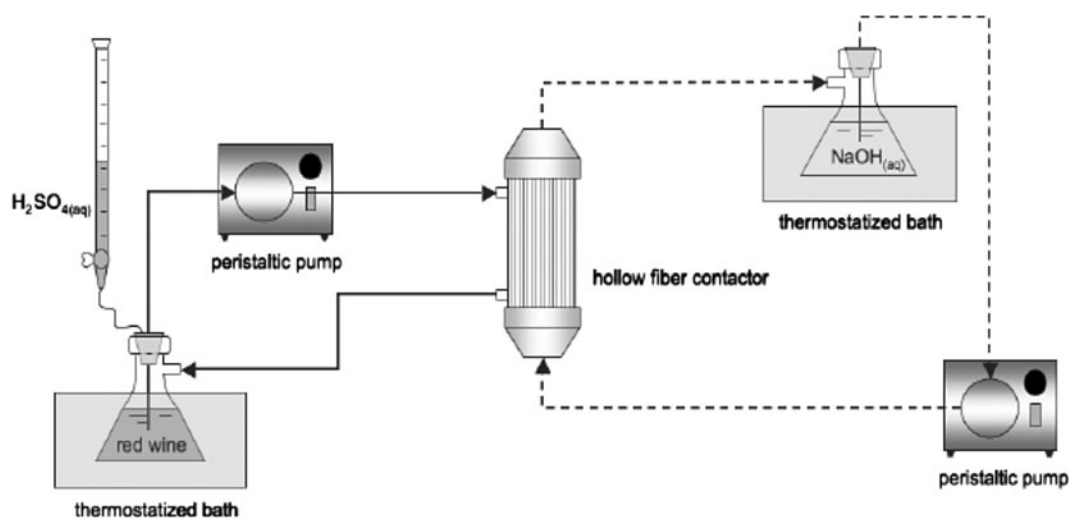


Fig. 4. Outline of the experimental setup used for the sulfite quantification in red wine [14].

sulfite compounds can be transferred through the membrane. For this reason, an acidification of the feed is necessary to ensure the formation of free sulfur dioxide.

Extraction tests were carried out both using wine-like model solutions containing Na_2SO_3 and Cabernet Sauvignon wines. Fig. 4 presents the experimental setup implied in this application, using the same configuration described in Fig. 2, but adapted at laboratory scale. The SO_2 removal is associated to a preliminary pH modification of the feed solution by adding H_2SO_4 , in order to increase the SO_2 availability during the extraction. The SO_2 content was monitored as a function of the time by means of continuous tests in the receiving solution applying the Ripper method.

Operating parameters of the applications described in the previous sections are summarized in Table 1.

3. General description of the mass transfer

The transfer of the volatile species through the membrane can be explained by means of a resistances-in-series model, which considers the transport phenomena at the proximities of the membrane. Thus, the transfer of the solute can be described by following sequence of steps: transfer from the bulk of the feed solution through the boundary layer to the feed–membrane interface, desorption of the solute, diffusion through the membrane pores filled with gas, absorption, and reaction in the receiving solution interface, and diffusion of the solute into the receiving solution.

3.1. Feed solution boundary layer

The feed flowed in the shellside for the ammonia removal and sulfite quantification applications and in the lumenside for the cyanide removal application.

The liquid mass transfer coefficient for the species i in the shellside, under laminar flow condition, can be calculated from the Sherwood correlation proposed by Prasad and Sirkar for the hollow fiber modules [15]:

$$Sh = 5.8 \left[\frac{D_h(1 - \phi)}{L} \right] \times Re^{0.6} \times Sc^{0.33} = \frac{K_f \times D_h}{D_{i,w}} \quad (6)$$

where D_h , ϕ , L , Re , Sc , $D_{i,w}$, K_f are the dynamic diameter of the shell, packing density, length of the fibers, Reynolds number ($Re = D_h u \rho / \mu$), Schmidt number ($Sc = \mu / \rho D_{i,w}$), the diffusion coefficient of the species i in water, and the mass transfer coefficient in feed side, respectively. The packing density can be calculated by means of Eq. (7).

$$\phi = N_F \left(\frac{d_e}{D_{in,s}} \right)^2 \quad (7)$$

where N_F represents the number of fibers, d_e is external diameter of the fibers, and $D_{in,s}$ is the internal diameter of the shell. Diffusion coefficient of the species i in water can be calculated from Wilke–Chang equation [23].

The liquid mass transfer coefficient for the species i in the lumenside, under laminar flow condition, can be calculated from the Sherwood correlation proposed by Leveque [24]:

$$Sh = 1.62 \left[\frac{d_{in}^2 v_l}{L \times D_{i,w}} \right]^{1/3} = \frac{K_f \times d_{in}}{D_{i,w}} \quad (8)$$

where v_l is the velocity of the feed in the lumenside of the hollow fibers and d_{in} is the inside diameter of the fiber.

The mass transfer coefficient in the feed side, K_f , can be predicted by using Eq. (6) or (8) due to the presence of the feed in lumen or shellside of the hollow fibers.

3.2. Desorption of the solute

The solute is desorbed from the feed–membrane interface. At the feed–membrane interface, the solute is considered in thermodynamic equilibrium with its vapor. In this way, Henry’s law may be applied at the interfaces. The partial pressure of species i can be calculated by the Eq. (9) using the Henry constant:

$$H = \frac{p_i}{c_i} \quad (9)$$

where p_i is the partial pressure of the species i in the air phase in equilibrium with the concentration c_i [mol m^{-3}] of this compound in the aqueous solution.

3.3. Transfer of the solute through the membrane pores

The membrane mass transfer coefficient, K_m , can be estimated from the following equation [15,25]:

$$K_m = \frac{\varepsilon D_{i,g}}{\tau \delta} \quad (10)$$

where $D_{i,g}$ is the diffusion coefficient of species i in the air gap within the pores while ε , τ , and δ are the porosity, the tortuosity, and the wall thickness of the hollow fiber, respectively. $D_{i,g}$ can be considered as either a molecular diffusion or the Knudsen diffusion

due to the value of Knudsen number ($Kn = \lambda/d_p$) [15], where λ is the molecular mean free path length and the d_p is the pore diameter. The Knudsen diffusion coefficient could be written as follows:

$$D_{kn} = \frac{d_p}{3} \left(\frac{8RT}{\pi M} \right)^{0.5} \quad (11)$$

where d_p is the pore diameter (cm), T the temperature in Kelvin (K), R is the universal gas constant ($\text{J mol}^{-1} \text{K}^{-1}$), and M is the molecular weight of the compound (g mol^{-1}).

The diffusion coefficient of the species i in the air gap, $D_{i,g}$ ($\text{m}^2 \text{s}^{-1}$), can be calculated using the correlation given by Fuller and coworkers or Chapman–Enskog equations given by Eqs. (12) and (13), respectively [26].

$$D_{i,g} = \frac{1 \times 10^{-7} T^{1.75} ((1/M_i) + (1/M_g))^{1/2}}{P \left[(\sum V_i)^{1/3} + (\sum V_g)^{1/3} \right]^2} \quad (12)$$

$$D_{i,g} = \frac{0.001858 T^{3/2} \times \sqrt{\frac{M_i + M_g}{M_i M_g}}}{P \times \sigma_{ig}^2 \times \Omega_{ig}} \quad (13)$$

The diffusion coefficients of ammonia and sulfite in air were estimated by the Fuller equation given by Eq. (12) and that of cyanide was estimated by the Chapman–Enskog equation given by Eq. (13).

3.4. Absorption and reaction in the receiving phase

For non-reactive receiving solutions, the mass transfer coefficients could be estimated from the Sherwood correlations given by Eq. (6) or (8) with respect to the flow configuration of the receiving solution in the hollow fiber module. However, the mass transfer coefficient in the receiving phase for a reactive strip solution is more difficult to predict. The mass transfer correlation depends on whether the reaction is fast or instantaneous reaction. The presence of the chemical reaction may significantly accelerate the rate of the mass transfer. The enhanced transfer rate is due to enhancement of the mass transfer coefficient and an increased driving force. When the concentration of the reactant in the receiving phase becomes higher relatively to the solvent, the reaction zone is expected to shift to the gas–liquid interface, and consequently, the reaction occurs on the interface of the membrane [27]. The reactions analyzed here between HCN and KOH, NH_3 and H_2SO_4 , and SO_2 and H_2SO_4 were supposed instantaneous [9–14,28–30] and were carried out in the

presence of excess amount of the reactant in the receiving solutions. Thus, as the volatile compound is absorbed by the receiving solution, it immediately reacts with the reactant in the receiving phase at the membrane-receiving solution interface and forms the nonvolatile by-product.

3.5. Transport in the receiving solution

The mass transfer of the solute is accelerated significantly by the chemical reaction. Thus, the mass transfer coefficient of the receiving solution side is much larger than the feed side mass transfer coefficient in the presence of a chemical reaction. When the reaction between the solute and the reactant is instantaneous, the concentration of the solute in the receiving solution is essentially zero. As the reaction occurs at the liquid–membrane interface very rapidly, it may be considered that there is no diffusion of the solute from the interface to the bulk of the receiving solution. Hence, the mass transfer resistance in the receiving solution side could be ignored and the overall mass transfer coefficient is given by Eq. (14):

$$\frac{1}{K} = \frac{1}{K_f} + \frac{1}{K_m} \quad (14)$$

3.6. Numerical solution of the model

Resistances-in-series model was solved estimating the interfacial concentration when the molar flow of the solute, N (mol s^{-1}), through the feed boundary layer and across the membrane pore represent the same flow values under instantaneous steady-state conditions as shown in Eq. (15):

$$N = K_f A_f (c_S^b - c_S^i) = K_m A_m c_{S,g}^i \quad (15)$$

in which c_S^b is the bulk concentration of the solute, c_S^i is the solute concentration on the interface of the membrane, and $c_{S,g}^i$ is the solute concentration in gas phase in equilibrium with that in solution on the interface, A_f is the membrane area of the feed side, and A_m is the logarithmic mean of the membrane area.

The Regula Falsi algorithm [31,32] was applied to reduce the number of iterative calculations, which have been achieved by means of a program developed in Matlab[®]. After these iterative calculations, the concentration of the solute in the bulk of the feed solution was recalculated by mass balance. Interfacial concentrations were estimated for each time interval by modifying the initial feed concentrations of each

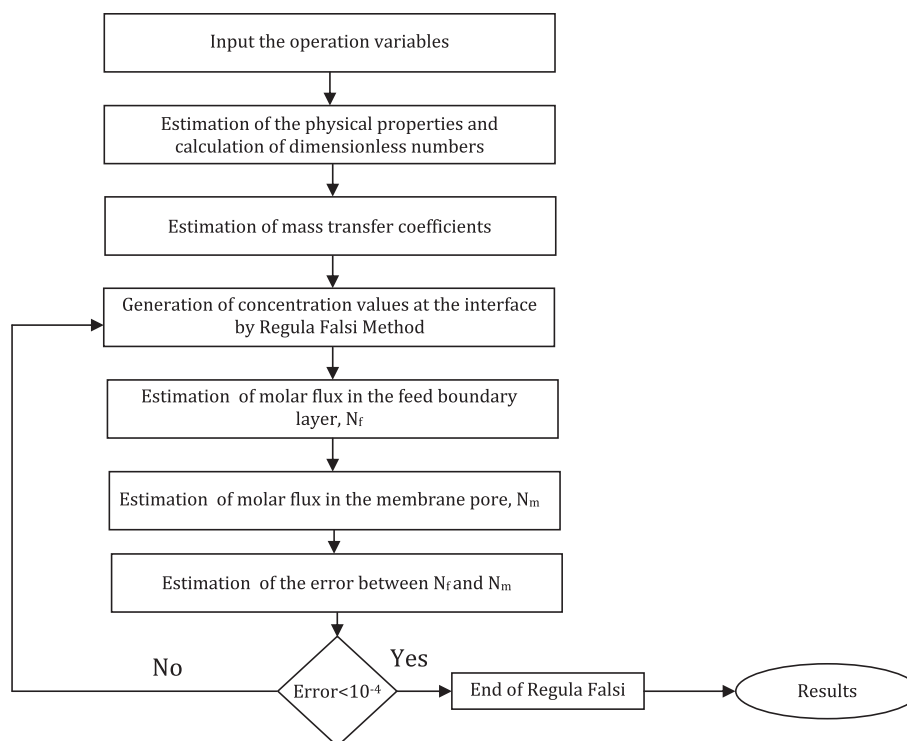


Fig. 5. Flowchart of the numerical solution.

corresponding step. The flowchart of the numerical solution is given in Fig. 5.

4. Results and discussion

4.1. Extraction performance and identification of the main mass transfer resistances

In all those experiments that were analyzed for the ammonia removal, a minimum extraction percentage of 98% was achieved in 35 min in a batch operation with a feed volume of 1,500 mL [9]. The best results were obtained with a diminution from an initial concentration of ammonia of 400 mg L^{-1} to a value of 2.5 mg L^{-1} ammonia that corresponds to 99.38% of ammonia removal. These results indicate that the destruction rate of the ammonia is very fast and the extraction percentage of the ammonia is significantly high. The chemical absorption was utilized drastically in terms of enhanced driving force for the mass transfer.

Fig. 6 presents a comparison of the fluxes obtained by experiments and the model predictions for the ammonia removal. Model predictions were calculated neglecting the receiving side mass transfer coefficient as described in Section 3.6. As can be seen in Fig. 6, the model and experimental results are in a good

agreement confirming that the mass transfer coefficient could be considered as a contribution of feed and membrane side resistances. The membrane mass transfer coefficients are much larger compared to the feed side mass transfer coefficients as can be

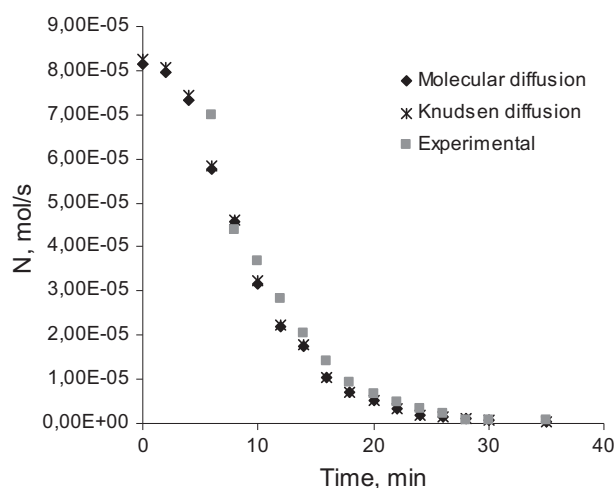


Fig. 6. Experimental and simulated values of molar flow as a function of the time; $[\text{H}_2\text{SO}_4] = 0.2 \text{ mol L}^{-1}$, $Q = 2000 \text{ mL min}^{-1}$, $T = 40^\circ\text{C}$, initial ammonia concentration is 500 ppm (Adapted from the work reported by Hasanoglu and coworkers [9]).

seen in Table 3. The percentages of the membrane mass transfer resistance over the total resistance are less than 1%, and therefore, the influence of the membrane mass transfer coefficient on the solute transport is very small. The Knudsen number of the hollow fiber was 0.38 for the ammonia molecules. As the Knudsen number is close to 1.0, the diffusion mechanism of ammonia inside the pores can be considered as a transition regime where various mechanisms could coexist. Therefore, ammonia diffusion through the pores could be described either by a molecular or a Knudsen like diffusion mechanism.

The hydrodynamic conditions of the hollow fiber contactor were analyzed in the previous work [9], showing a comparison of the concentration change with time for two cases where the feed solution was circulated in the lumenside and in the shellside. Extraction percentages of ammonia were higher when the feed solution flowed in the shellside and the acid solution in the lumenside of the membranes. These results indicate that the hydrodynamic conditions have a strong influence on the mass transfer resistances for this system. A clear difference was observed comparing both configurations of circulations because the mass transfer coefficient of the feed side that controls the overall transfer is strongly modified when the circulation of solutions is changed. These results confirm that the feed boundary layer has a strong influence on the mass transfer through the membrane.

Previous studies in the literature have investigated the removal of ammonia using gas-filled membrane absorption [28–30]. Zhu and coworkers [28] reported a study in order to investigate the effect of the pH and the viscosity of the wastewater containing ammonia on the mass transfer in hydrophobic hollow fiber membrane contactors. In the reported work, the removal efficiency of ammonia was over 98% in 40 min when the initial pH values of the feed solution

were over 11. Tan and coworkers [29] reported a work for ammonia removal from water through polyvinylidene fluoride hollow fiber membranes. It has been indicated that increased pH values allowed higher efficiencies of ammonia removal, and remarkable efficiencies have been reached when the pH value was higher than 11 after a time period of 120 min. Nordahl and coworkers [30] reported that the relative effect of temperature on ammonia mass transfer rates was noticeably higher at pH values exceeding 10, while the noticeable efficiencies were performed about in 100 min. The reported studies show that the choice of the pH value of feed might be an important variable on the removal efficiency of the process since the presence of the volatile form of the species is usually dominated by pH value of the feed.

From the results of SO₂ extraction from liquid solutions, Fig. 7 presents the comparison of the extraction percentages of the experimental and model results. Significantly high values of extraction percentages were obtained (up to 99.2%) with the experiments. It was possible to obtain an average extraction percentage of 98.91%, after four minutes processing 300 mL of feed solutions. The extraction of SO₂ from the wine samples was achieved very fast and well controlled by means of chemical membrane absorption. The theoretical results were obtained on the base of both molecular and Knudsen diffusion equations. The predictions are in good agreement with the experimental results indicating that the mass transfer in the pores could be described by either molecular diffusion or Knudsen diffusion.

The experimental results of HCN extraction reported by Xu and coworkers [11] indicate that the cyanide removal rate was very high for the artificial wastewater. The cyanide concentration rapidly decreased to 205.9 mg L⁻¹ from 1277.5 mg L⁻¹, and 83.9% cyanide was removed within the first 20 min. After 90 min of operation, 99.9% of cyanide was

Table 3
Feed side and membrane mass transfer coefficients of each analyzed system and Henry's constants of the solutes

System	Application	Temperature (°C)	Henry's constant of the solute (Pa m ³ mol ⁻¹) [32–35]	Mass transfer coefficient in the feed boundary layer, K_f (m s ⁻¹)	Mass transfer coefficient in the membrane, K_m (m s ⁻¹)
1	NH ₃ removal from water	40	3.479	4.600×10^{-6}	1.660×10^{-1}
2	HCN removal from wastewater	20	8.323	1.134×10^{-5}	4.430×10^{-2}
3	SO ₂ quantification from wines and fruit juices	27	78.899	7.510×10^{-6}	5.060×10^{-2}

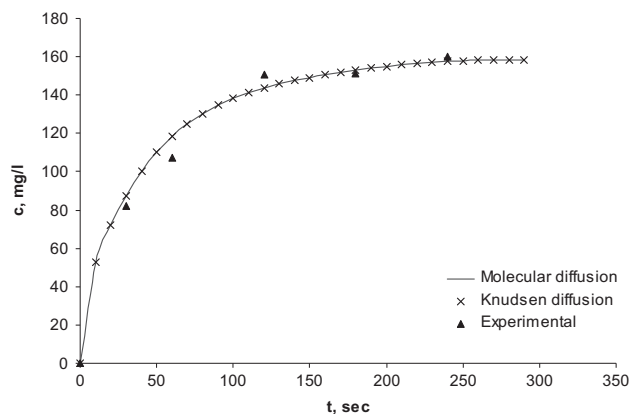


Fig. 7. Experimental and simulated values of concentration of SO_2 in the extraction solution as a function of the time ($Q_{\text{shell}} = 1.45 \text{ L min}^{-1}$, $Q_{\text{fiber}} = 1.20 \text{ L min}^{-1}$, $T = 27^\circ\text{C}$).

removed and the cyanide concentration dropped to below 0.5 mg L^{-1} . At the end of the process, 98% of the cyanide was recovered. In this work, the experimental data of Xu and coworkers [11] were simulated using the unified approach for the gas-filled membrane absorption described in above sections, which involves an instantaneous reaction on the interface of the membrane. According to this model, the overall mass transfer resistance included the feed liquid film resistance and the membrane resistance since the resistance of stripping side was neglected. Calculations were made as it was described in Section 3.6. Fig. 8 represents a comparison of experimental data of Xu and coworkers and the calculated concentrations vs. time. The proposed model for the process satisfied with the data of those obtained from experimental work of Xu and coworkers. As can be seen in Fig. 8, similar to ammonia and sulfur dioxide cases (Figs. 6 and 7), there was not a distinct difference between the data calculated from two diffusion mechanisms indicating that the transfer in the pores could be described as Knudsen or molecular diffusion. Furthermore, the diffusion of the gaseous HCN in the pores is the equivalent to that in air, which is much faster than that in water. Thus, the contribution of the membrane resistance to the overall resistance is not remarkable and feed side resistance mainly determines the overall resistance. On the other hand, this is not unexpected because the thickness of the gas gap is relatively small, which could be between 20 to 40 μm .

4.2. Effect of the chemical absorption on the performance of the process

The presence of the chemical reaction in gas-filled membrane absorption processes enhances the mass

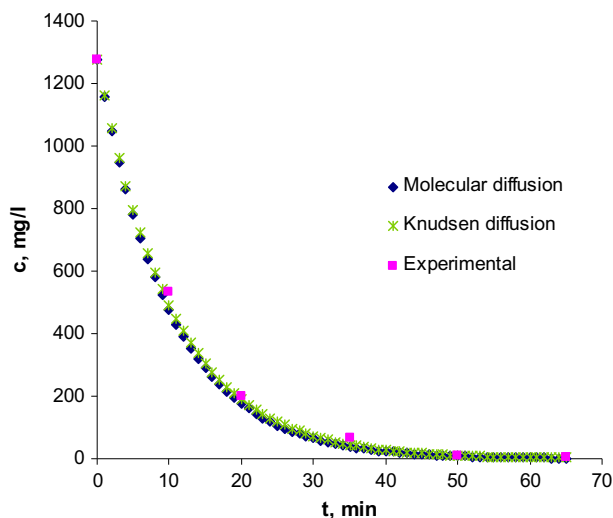


Fig. 8. Experimental [11] and simulated values of the concentration of cyanide as a function of the time.

transfer rate of the species to be removed. Thus, the driving force for the mass transfer increases that leads to an efficient separation process. In case of the excess amount of the reactant in the receiving solution, the reaction zone seems to be placed on the interface of the membrane. This fact can be confirmed by the extraction efficiency of the three processes analyzed in this work through the results reported in Figs. 6–8, which show similar behavior in spite of the fact that they present three different reactions. The faster extraction rate in the case of SO_2 removal is directly related to the higher Henry's constant value reported in Table 3.

On the other hand, the main common aspect in the studied applications is the hydrodynamic condition, since hollow fiber contactors were used. These three different systems may be described by means of the same approach taking into account a negligible vapor pressure of the volatile compound in the receiving side. Eqs. (1) to (4) give the corresponding absorption reactions of ammonia, sulfur dioxide, and cyanide with their reactive receiving solutions, where the reactants in the receiving solutions were sulfuric acid, NaOH, and KOH, respectively. Thus, the chemical reactions, under the operation conditions applied in these experiments, do not modify the behavior of the transfer rate in the studied processes where the main parameters to be considered are the mass transfer coefficients of the volatile compound through the liquid feed boundary layer and the pore filled with gas, as well as the Henry's constant to quantify the equilibrium conditions at the pore entrance. Table 3 presents the Henry's constants of the solutes and the

mass transfer coefficients in the feed boundary layer and in the membrane pore for each analyzed system.

4.3. Effect of the chemical kinetics in the membrane absorption process

The simulations reported in Figs. 6–8 have been done considering instantaneous reactions and any effect of the receiving phase boundary layer. In order to verify the influence of the conditions in the receiving solution on the extraction rate, the effect of the concentration of receiving solution was investigated for the case of ammonia removal and its results were reported in our previous work [9]. Although a slight decrease in the extraction percentages were observed within the first 15 min, the influence of the acid concentration was not significant for the total time of the extraction, since the acid concentration was in excess compared to ammonia content in the feed.

The Hatta number (Ha), a dimensionless quantity, is useful in evaluating the kinetic regime describing the effect of chemical reaction on the mass transfer rate. The Hatta number is defined as the ratio of diffusion time to the reaction time. In case of an irreversible second-order reaction, species A and B are converted in the liquid phase into one or more products where the reaction, reaction rate, and Hatta number are as follows:



$$R_A = k_R C_B C_A \quad (17)$$

$$Ha = \sqrt{\frac{k_R C_{B,0} D_A}{k_l}} \quad (18)$$

In this case, not only species A has to diffuse in the liquid layer, but also species B. This introduces an extra parameter, the maximum enhancement factor, which is approximately given by the equation below [36,37]:

$$E_\infty = \left(1 + \frac{c_{B,0} D_B}{\nu_B c_{A,i} D_A}\right) \left(\frac{D_A}{D_B}\right)^n \quad (19)$$

The value of n depends on the mass transfer model chosen. In the current case where a boundary layer flow is present, the value of n is 1/3.

Approximate reaction rate constants of the investigated reactions are taken from the literature [38–40] and Ha number and E_∞ are estimated and given in Table 4:

Table 4
Parameters for Hatta estimations

System	k_R , L mol ⁻¹ s ⁻¹	E_∞	Ha number
NH ₃ –H ₂ SO ₄ solution	1.14×10^8	9	26.1
HCN–KOH solution	3.70×10^9	58	103.1
SO ₂ –NaOH solution	2.89×10^8	9.3	13.6

The rate of a reaction can be determined from the value of the Hatta number. When $Ha > 2$, the reaction is considered to be fast, while if $Ha \gg E_\infty$, the reaction is instantaneous indicating that the mass transfer coefficient may be increased significantly by the presence of the reaction [36,37]. For all three cases of reaction systems, the condition of $Ha \gg E_\infty$ is satisfied and accordingly, the absorption regime over the entire fiber can be assumed as instantaneous reaction regime. Thus, it can be concluded that the kinetic regime of the analyzed reactions is instantaneous and, therefore, resistance of the reactive solution boundary layer to mass transfer can be neglected indicating that interfacial reaction does not dominate the solute transfer.

In case of an instantaneous reaction with an excess amount of reactant in the receiving solution, it is theoretically possible to remove the entire undesired volatile compound in the feed since the vapor pressure of the species in the receiving side could be essentially zero and consequently, the driving force would have the maximum value. Under this configuration, the magnitude of the concentration gradient across the membrane is controlled by Henry's law coefficient of the species that diffuses through the membrane. The balance of distribution of a compound between a liquid and a gas phase depends on the affinities of the substance for both phases as well as on the factors such as concentration, temperature, pH, reactivity, and solubility where this process is characterized by the Henry's law coefficient of the compound. The concentration gradient across the membrane will increase with the increase of vapor pressure of the volatile compound in the feed solution to be treated, which is strongly dominated by Henry's law coefficient.

The effect of the chemical kinetic in the receiving phase from volatile to non-volatile species does not seem to be significant in the studied cases, since receiving phases were not diluted and its solute represented the excess reactants. It could be possible to observe the effect of the chemical kinetic, if the concentration of the receiving solution were lower in terms of stoichiometry with the feed solution, but this was not found in the literature for any of the studied systems.

5. Conclusions

A membrane-based methodology of the so-called gas-filled membrane absorption has been described by analyzing three applications of this process with a common approach. The described process is based on coupled physical and chemical phenomena that can allow practically the total extraction of a specific compound in the feed with the use of a reactive strip solution. High extraction percentages can be achieved even at very low concentrations in the feed. This result may be very advantageous for some specific applications of wastewater treatments, food applications or design of new, compact, and efficient operations to be applied in different fields.

Henry's law coefficient of the species to be separated is an important parameter of this process since it controls the size of the concentration gradient across the membrane. Furthermore, some of the volatile compounds dissociate in aqueous solutions, and therefore, they may be in presence in the form of various species in aqueous solutions where the concentrations of this species are dominated by pH. Thus, the balance of distribution of a compound between a liquid and a gas phase may also be characterized by the pH value relative to its dissociation affinity. Therefore, the pH value of the feed is found to have an important effect on the mass transfer through the membrane for those volatile compounds that are easily ionized.

Overall mass transfer coefficient is contributed by both the feed side and the membrane mass transfer coefficients, but in different quantities, substantially by the feed side mass transfer coefficient. Therefore, it can be concluded that the transport across the membrane is mainly controlled by the feed side boundary layer. The resistance from the strip side mass transfer coefficient may be neglected taking into account the chemical absorption in this phase. On the base of the unified approach proposed in this study, the overall mass transfer coefficient could be predicted using the empirical correlations from literature. The proposed approach considers a resistance-in-series model based on a group of mass transport equations, which has been applied to explain experimental data of HCN removal reported by Xu and coworkers [11]. This model has been proposed to predict the experimental data of ammonia removal in a previous work [9] and also applied to the sulfite removal for its quantification by means of a similar membrane absorption process. All the experimental data of the three analyzed cases are in good agreement with its modeling results. This modeling methodology could be used to extrapolate or to scale-up this type of systems. Furthermore, the consistent behavior of the analyzed cases under

the same configuration involving an instantaneous reaction of the solute through a reactive receiving solution indicates that this methodology could be proposed for an efficient extraction, transformation or quantification of many volatile compounds or dissolved gasses from aqueous streams.

The use of gas-filled membrane absorption to remove the volatile compounds/dissolved gases by means of a reactive stripping solution offers several advantages over conventional methods: no secondary pollutants are produced, by-product can be generated and recovered, the operation cost is low, fast separation and high extraction percentages can be achieved.

Acknowledgments

The financial support of Project FONDECYT 1100305 (CONICYT Chile) and postdoctoral program of VRID/USACH for A. Hasanoglu are gratefully acknowledged.

Nomenclature

A_f	—	membrane area of the feed side (m^2)
A_m	—	logarithmic mean of the membrane area (m^2)
c	—	concentration (mg L^{-1})
c_s^b	—	solute concentration of the bulk solution (mol m^{-3})
c_s^i	—	solute concentration on the interface of the membrane (mol m^{-3})
$c_{s,g}^i$	—	solute concentration in gas phase in equilibrium with that in solution on the interface (mol m^{-3})
$D_{i,g}$	—	molecular diffusion coefficient of the species i in air ($\text{m}^2 \text{s}^{-1}$)
$D_{i,w}$	—	diffusion coefficient of the species i in water ($\text{m}^2 \text{s}^{-1}$)
d_e	—	external diameter of the fiber (m)
D_H	—	dynamic diameter (m)
d_{in}	—	internal diameter of the fiber (m)
$D_{in,s}$	—	internal diameter of the shell (m)
D_{kn}	—	Knudsen diffusion coefficient ($\text{m}^2 \text{s}^{-1}$)
d_p	—	pore diameter of the membrane (cm)
H	—	Henry's constant ($\text{Pa m}^3 \text{mol}^{-1}$)
K_f	—	mass transfer coefficient in the feed side (m s^{-1})
K_m	—	mass transfer coefficient in the membrane pores (m s^{-1})
K_{ov}	—	overall mass transfer coefficient (m s^{-1})
k_R	—	reaction rate ($\text{L mol}^{-1} \text{s}^{-1}$)
L	—	length of the fiber (m)
M	—	molecular weight of the compound (g mol^{-1})

M_i, M_g	—	molecular weight of i and gas (air) (g mol^{-1})
N_F	—	number of fibers
P	—	pressure (Pa)
p_i	—	partial pressure of specie i (Pa)
R	—	universal gas constant ($\text{J mol}^{-1} \text{K}^{-1}$)
Q	—	flow rate of the solution (mL min^{-1})
u	—	velocity of the solution (m s^{-1})
T	—	temperature in Kelvin (K)
V_i, V_g	—	molecular volumes of specie i and gas (air), respectively (g cm^{-3})

Greek symbols

δ	—	wall thickness of the membrane (m)
ε	—	porosity
τ	—	tortuosity
ϕ	—	packing density
λ	—	molecular mean free path length (m)
μ	—	viscosity ($\text{kg m}^{-1} \text{s}^{-1}$)
ρ	—	density (kg m^{-3})
σ_{ig}	—	collision diameter, Å
Ω_{ig}	—	collision integral, dimensionless

References

- [1] L. Rui, X. Jun, W. Lianjun, L. Jiansheng, S. Xiuyun, Reduction of VOC emissions by a membrane-based gas absorption process, *J. Environ. Sci.* 21 (2009) 1096–1102.
- [2] C. Guizard, B. Boutevin, F. Guida, A. Ratsimihety, P. Ambard, J.C. Lasserre, S. Naiglin, VOC vapour transport properties of new membranes based on cross-linked fluorinated elastomers, *Sep. Purif. Technol.* 22–23 (2001) 23–30.
- [3] D.J. Kim, H. Kim, Degradation of toluene vapor in a hydrophobic polyethylene hollow fiber membrane bioreactor with *Pseudomonas putida*, *Process Biochem.* 40 (2005) 2015–2020.
- [4] T.K. Poddar, S. Majumdar, K.K. Sirkar, Removal of VOCs from air by membrane-based absorption and stripping, *J. Membr. Sci.* 120 (1996a) 221–237.
- [5] T.K. Poddar, S. Majumdar, K.K. Sirkar, Membrane-based absorption of VOCs from a gas stream, *AIChE J.* 42 (1996b) 3267–3282.
- [6] F. Wiesler, Ultrapure water, Technical Report UP130427 (1996) 27–31.
- [7] Y. Lv, X. Yu, S.T. Tu, J. Yan, E. Dahlquist, Wetting of polypropylene hollow fiber membrane contactors, *J. Membr. Sci.* 362 (2010) 444–452.
- [8] J. Romero, G.M. Rios, J. Sanchez, Analysis of boundary layer and solute transport in osmotic evaporation, *AIChE J.* 49 (2003) 2783–2792.
- [9] A. Hasanoglu, J. Romero, B. Pérez, A. Plaza, Ammonia removal from wastewater streams through membrane contactors: Experimental and theoretical analysis of operation parameters and configuration, *Chem. Eng. J.* 160(2) (2010) 530–537.
- [10] Z. Shen, J. Huang, G. Qian, Recovery of cyanide from wastewater using gas-filled membrane absorption, *Water Environ. Res.* 69 (1997) 363–397.
- [11] Z. Xu, L. Li, Z. Shen, Treatment of praziquantel wastewater using the integrated process of coagulation and gas membrane absorption, *Water Res.* 39 (2005) 2189–2195.
- [12] B. Han, Z. Shen, S.R. Wickramasinghe, Cyanide removal from industrial wastewaters using gas membranes, *J. Membr. Sci.* 257 (2005) 171–181.
- [13] Z. Shen, B. Han, S.R. Wickramasinghe, Cyanide removal from industrial praziquantel wastewater using integrated coagulation-gas-filled membrane absorption, *Desalination* 195 (2006) 40–50.
- [14] A. Plaza, J. Romero, E. Morales, B. Perez, W. Silva, Membrane-based ripper method to accurate determination of free and bonded sulfite content in red wine, *Euromembrane 2009*, The EMS Conference, 6–10 September 2009, France.
- [15] A. Gabelman, S. Hwang, Hollow fiber membrane contactors, *J. Membr. Sci.* 159 (1999) 61–106.
- [16] B.W. Reed, M.J. Semmens, E.L. Cussler, Membrane contactors, *Membr. Sci. Technol.* 2 (1995) 467–498.
- [17] R. Klaassen, P. Feron, A. Jansen, Membrane contactor applications, *Desalination* 224 (2008) 81–87.
- [18] R. Klaassen, P. Feron, A. Jansen, Membrane contactors in industrial applications, *Chem. Eng. Res. Des.* 83 (2005) 234–246.
- [19] A. Mansourizadeh, A.F. Ismail, Hollow fiber gas-liquid membrane contactors for acid gas capture: A review, *J. Hazard. Mater.* 171 (2009) 38–53.
- [20] Z. Lazarova, B. Syska, K. Schügerl, Application of large-scale hollow fiber membrane contactors for simultaneous extractive removal and stripping of penicillin G, *J. Membr. Sci.* 202 (2002) 151–164.
- [21] R.S. Juang, C.Y. Wu, Microbial degradation of phenol in high-salinity solutions in suspensions and hollow fiber membrane contactors, *Chemosphere* 66 (2007) 191–198.
- [22] Z.G. Penga, S.H. Lee, T. Zhou, J.J. Shieh, T.S. Chung, A study on pilot-scale degassing by polypropylene (PP) hollow fiber membrane contactors, *Desalination* 234 (2008) 316–322.
- [23] C.J. Geankoplis, *Transport processes and unit operations*, third ed. Prentice Hall PTR, Englewood Cliffs, NJ, 1993.
- [24] A. L ev eque, Les lois de la transmission de chaleur par convection (The heat transfer laws by convection), *Ann. Mines.* 13 (1928) 201–299.
- [25] H. Mahmud, A. Kumar, R.M. Narbaitz, T. Matsuura, A study of mass transfer in the membrane air-stripping process using microporous polypropylene hollow fibers, *J. Membr. Sci.* 179 (2000) 29–41.
- [26] D. Green, R. Perry, *Perry's Chemical Engineer's Handbook*, eighth ed. McGraw Hill, New York, NY, 2007.
- [27] Kang Li, *Ceramic Membranes for Separation and Reaction*, John Wiley & Sons, Chichester, 2007.
- [28] Z. Zhu, Z. Hao, Z. Shen, J. Chen, Modified modeling of the effect of pH and viscosity on the mass transfer in hydrophobic hollow fiber membrane contactors, *J. Membr. Sci.* 250 (2005) 269–276.
- [29] X. Tan, S.P. Tan, W.K. Teo, L. Lia, Polyvinylidene fluoride (PVDF) hollow fibre membranes for ammonia removal from water, *J. Membr. Sci.* 271 (2006) 59–68.
- [30] B. Norddahl, V.G. Horn, M. Larsson, J.H. Preez, K. Christensen, A membrane contactor for ammonia stripping, pilot scale experience and modeling, *Desalination* 199 (2006) 172–174.
- [31] A. Quarteroni, *M ethodes num eriques pour le calcul scientifique (Numerical methods for scientific calculation)*, Springer, Paris, 2000.
- [32] H. Vald es, J. Romero, A. Saavedra, A. Plaza, V. Bubnovich, Concentration of noni juice by means of osmotic distillation, *J. Membr. Sci.* 330 (2009) 205–213.
- [33] R. Sander, *Compilation of Henry's law constants for inorganic and organic species of potential importance in environmental chemistry* (1999). Available from: <http://www.mpch-mainz.mpg.de/~sander/res/henry.html>.
- [34] D. Dzombak, R. Ghosh, G. Wong-Chong, *Cyanide in Water and Soil: Chemistry, Risk and Management*. Taylor and Francis Group, Boca Raton, FL, 2006.
- [35] M. Mondal, Experimental determination of dissociation constant, Henry's constant, heat of reaction, SO₂ absorbed and gas bubble—liquid interfacial area for dilute sulphur dioxide absorption into water, *Fluid Phase Equilib.* 253 (2007) 98–107.
- [36] A. Mansourizadeh, A.F. Ismail, Hollow fiber gas-liquid membrane contactors for acid gas capture: A review, *J. Hazard. Mater.* 171(1–3) (2009) 38–53.

- [37] P.S. Kumar, J.A. Hogendoorn, P.H.M. Feron, G.F. Versteeg, Approximate solution to predict the enhancement factor for the reactive absorption of a gas in a liquid flowing through a microporous membrane hollow fiber, *J. Membr. Sci.* 213 (2003) 231–245.
- [38] M. Schultes, Absorption of sulfur dioxide with sodium hydroxide solution in packed columns, *Chem. Eng. Technol.* 21 (1998) 201–209.
- [39] B.H. Baek, V.P. Aneja, Q. Tong, Chemical coupling between ammonia, acid gases, and fine particles, *Environ. Pollut.* 129 (2004) 89–98.
- [40] D.W. Oxtoby, H.P. Gillis, A. Campion, *Principles of Modern Chemistry*, 7th ed. Brooks/Cole Cengage Learning, Belmont, CA, 2011.